TRANSIENT AND LONG-TERM DISPLACEMENT-LENGTH SCALING OF PLANETARY FAULTS. Richard A. Schultz and Amanda L. Nahm, Geomechanics–Rock Fracture Group, Department of Geological Sciences and Engineering/172, University of Nevada, Reno, NV 89557–0138, schultz@mines.unr.edu, www.mines.unr.edu/geo-eng/schultz.

Summary: Displacement-length (*D-L*) measurements for the largest planetary faults, including lithospheric-scale thrust faults on Earth (Fig. 1), Mars, and Mercury, are consistent with linear *D-L* scaling relations [1,2]. This scaling relation requires that the faults grow self-similarly in length and down-dip height [3], in apparent violation of restriction at depth by either stratigraphy or rheology (i.e., seismogenic depth). Approximately self-similar growth of faults across stratigraphic and rheologic horizons is, however, well known for many terrestrial fault systems, while restriction of earthquakes by temperature, and faults by stratigraphy, is also well documented. Here we differentiate between transient, temporal controls on fault displacements and long-term scaling relations for surface-breaking planetary faults.

Basic Observations: Data from terrestrial normal, strike-slip, and thrust faults demonstrate linear *D-L* scaling relations over a wide range of length scales [e.g., 1,4,5] (Fig. 1). We suggest that the issue of whether the faults were transiently restricted at depth may be assessed from comparing the scaling relation to individual fault displacement profiles.

Dawers et al. [6] showed that normal faults that cut non-welded Bishop Tuff defined a linear *D-L* scaling relation (Fig. 2). However, they also demonstrated that the displacement profiles defined two basic groups: smaller faults having peaked or triangular displacement profiles and longer faults having more flat-topped, plateaued profiles. Faults longer than ~twice the 150-m thickness of the tuff (dashed line at L = 300 m) showed plateaued profiles, suggesting their restriction to the tuff sequence and in apparent violation of the linear *D-L* scaling relation (Fig. 2) and cumulative length-frequency statistics [7].

Field observations, both in map view and in cross section, and measurements by *Soliva et al*. [8] demonstrate that stratigraphically restricted faults are characterized by flat-topped displacement profiles. The *D-L* scaling relations of these demonstrably stratigraphically restricted faults follow shallower, nonlinear paths on the *D-L* diagram (Fig. 3). Comparable growth paths have recently been identified for Martian grabens that also show plateaued displacement profiles and uniform cross-strike spacings [9] (see Fig. 3b). However, as noted by [8], fault restriction is transient, with up- and down-dip propagation occurring as fault strain continues to accumulate. Resulting fault shapes in such layered sequences are more rectangular than elliptical, as documented in seismic profiling of faults in terrestrial sedimentary basins [10].

Populations of earthquakes define two basic groups depending on whether they rupture the entire seismogenic thickness or not [e.g. 11,12] and their scaling relations, from “small” to “large” events, can be well characterized

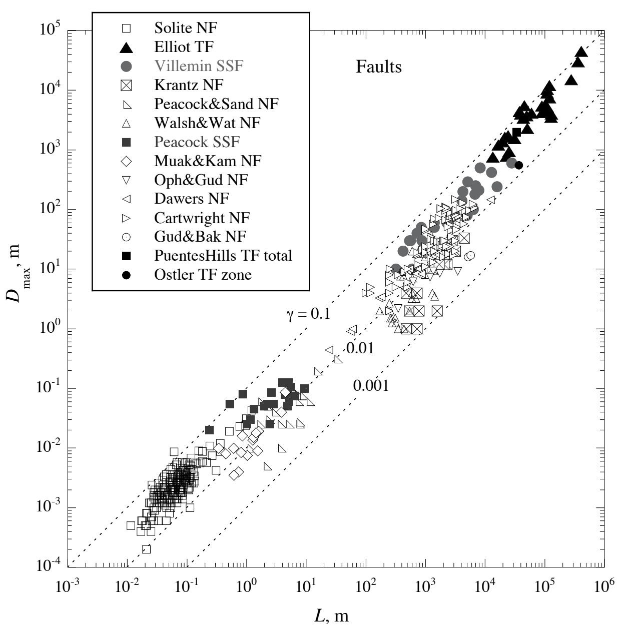

Fig. 1. Displacement-length relations for terrestrial faults, after *Schultz et al*. [1]. Note consistency of individual datasets with linear *D-L* scaling (dotted lines in the figure).

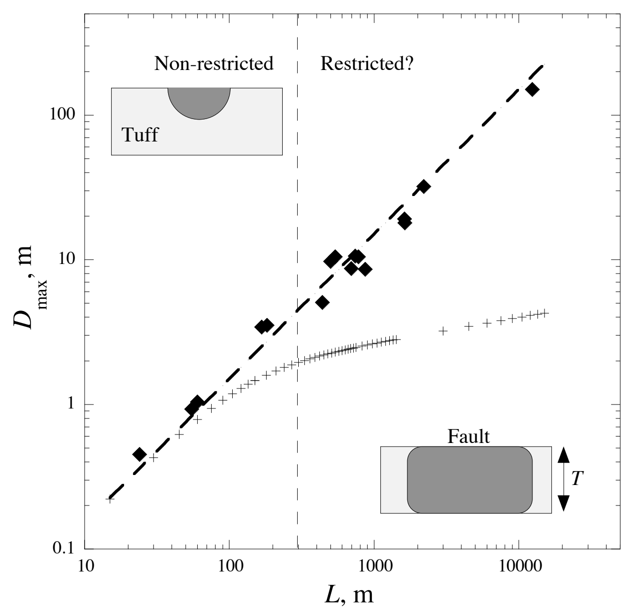

Fig. 2. Displacement-length relations for normal faults in Bishop Tuff, after *Dawers et al*. [6]. Linear *D-L* scaling is indicated by the dashed line; lower curve corresponds to restricted faults [3] predicted for T = 150 m and fault aspect ratio L/H = 2.

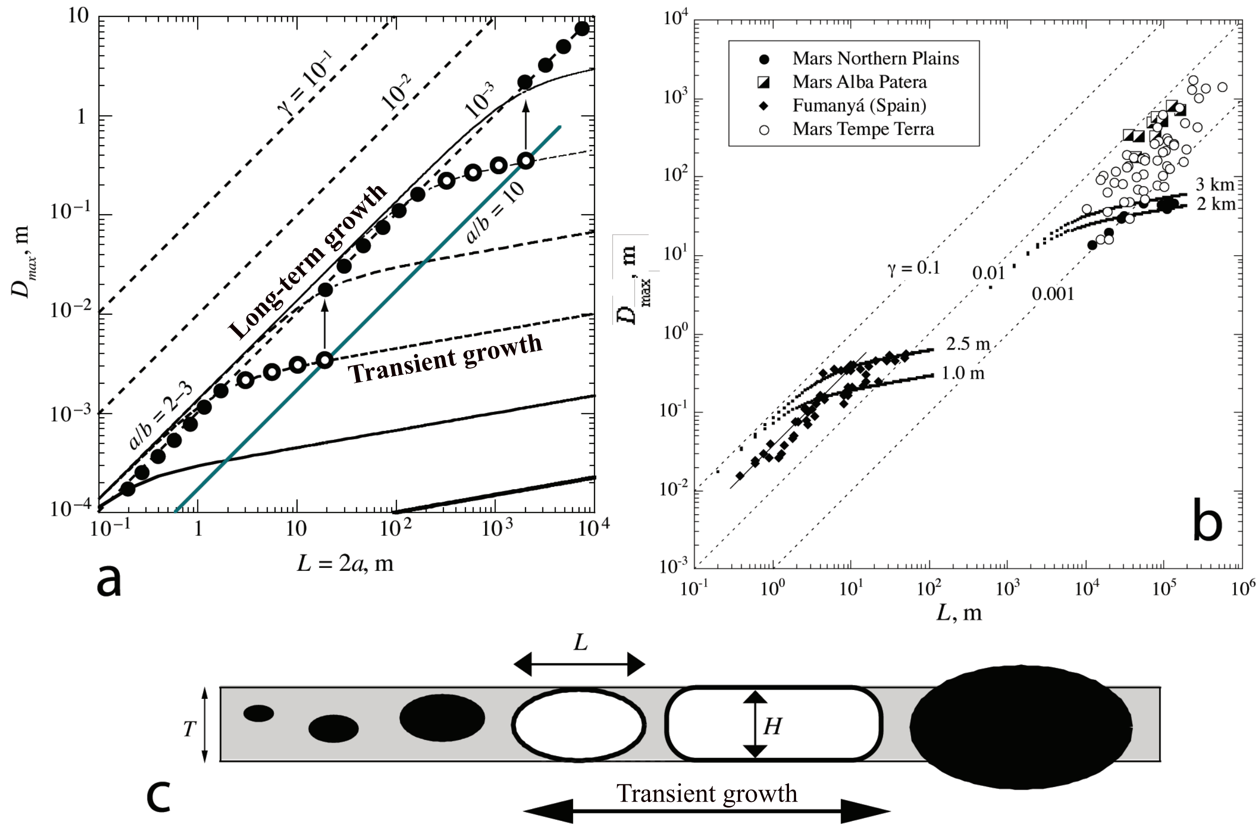

Fig. 3. Displacement-length relations for faults, after [3,18]. 3-D displacement-length scaling relations and the growth of stratigraphically restricted faults. (a) Fault growth paths on the D_{max}-L diagram showing stair-step trajectory of alternating transient excursions (restricted, open symbols)) from long-term (linear, filled symbols)) fault growth. (b) Examples of restricted fault populations on Earth (normal faults from Fumanyá in the southeast Pyrenees, after [8]) and Mars (graben-bounding normal faults from the northern plains, after [9]). (c) Cross-sectional fault geometries shown schematically for each part of the growth sequence. Filled and open symbols for fault-shape ellipses as in (a).

by using the relationship given by [3] (see [13]). The topography of surface-breaking faults is closely related to the distribution of coseismic slip at depth [e.g., 14], implying a correspondence between the fault displacement distribution and seismogenic layer thickness. However, the seismic cycle, and therefore the accumulation of displacements along a fault, is not complete without explicitly considering stable creep along the fault at depths greater than the lower stability transition during the interseismic period [e.g., 15,16].

Transient vs. Long-Term Scaling and Implications for *D-L* Scaling of Planetary Faults: Stratigraphic or rheologic restriction of faults on planetary surfaces can be inferred if their displacement distributions are plateaued *and* if their *D-L* scaling relations are nonlinear. Previously (or transiently) restricted faults would be indicated by plateaued distributions and linear *D-L* scaling, as appears to be the case for the normal faults in Bishop Tuff studied by *Dawers et al*. [6]. Detailed observations of normal faults in Afar (Africa [17]) and Alba Patera (Mars [9]) are consistent with fault growth, both along-strike and down-dip, with rapid displacement accumulation associated with the cessation of restriction at depth and a return to linear *D-L* scaling. Because the duration of transient excursions from the long-term linear scaling relationship depends on the yield strength contrast between the restricting layer and its surroundings [8], the degree of departure from linear *D-L* scaling provides a probe of crustal properties over the lifetimes of planetary faults.

References: [1] Schultz et al. (2006) *JSG*, **28**, 2182–2193. [2] Watters et al. (2002) *GRL*, **29**, 10.1029/2001GL014308. [3] Schultz and Fossen (2002) *JSG*, **24**, 1389–1411. [4] Cowie and Scholz (1992) *JSG*, **14**, 1149–1156. [5] Clark and Cox (1996) *JSG*, **18**, 147–152. [6] Dawers et al. (1993) *Geology*, **21**, 1107–1110. [7] Scholz et al. (1993) *JGR*, **98**, 21,951–21,961. [8] Soliva et al. (2005) *GRL*, **32**, 10.1029/2005GL023007. [9] Polit et al. (2009) *JSG*, in press. [10] Benedicto et al. (2003) *GRL*, **30**, 10.1029/2003GL018237. [11] Scholz (1982) *BSSA*, **72**, 1–14. [12] Scholz (2002) *The Mechanics of Earthquakes and Faulting*, Cambridge Univ. Press. [13] Wilkins and Schultz (2005) *BSSA*, **95**, 2232–2258. [14] Cohen (1999) *Adv. Geophys*., **41**, 133–231. [15] Tse and Rice (1986) *JGR*, **91**, 9452–9472. [16] Marone (1998) *Annu. Rev. Earth Planet. Sci*., **26**, 643–696. [17] Soliva and Schultz (2008) *Tectonics*, **27**, 10.1029/2007TC002148. [18] Schultz et al. (2009) Fault populations, in *Planetary Tectonics*, Cambridge Univ. Press, in press.

Abstract published in *Lunar and Planetary Science*, *XL*, CD-ROM (www.lpi.usra.edu/meetings), Lunar and Planetary Institute, Houston (2009).